International Journal of Heat and Mass Transfer 113 (2017) 730–740

Contents lists available at ScienceDirect

International Journal of Heat and Mass Transfer

journal homepage: www.elsevier.com/locate/ijhmt

Understanding of spatter formation in fiber laser welding of 5083 aluminum alloy

Dongsheng Wu, Xueming Hua *, Fang Li, Lijin Huang

[a] Shanghai Key Laboratory of Material Laser Processing and Modification (Shanghai Jiaotong University), Shanghai 200240, PR China
[b] Collaborative Innovation Center for Advanced Ship and Deep-Sea Exploration, Shanghai 200240, PR China

ARTICLE INFO

Article history:
Received 19 September 2016
Received in revised form 5 May 2017
Accepted 28 May 2017

Keywords:
Laser welding
Keyhole
Spatter
CFD

ABSTRACT

The droplet escape condition is established, a three-dimensional numerical model is built to investigate the behavior of the weld pool in fiber laser welding of 5083 aluminum alloy, the shear stress caused by the metallic vapor flow that has great influence on spatter formation is considered. A high speed photography system is used to capture the transient images of the weld pool, the spatter formation is discussed. The numerical and experimental results show that the spatters generate mainly around the keyhole. Two factors are responsible for the spatter formation: the surface tension of the molten metal around the keyhole is low. The recoil pressure caused by evaporation and the shear stress caused by metallic vapor flow accelerate the upward moving melt around the keyhole. Increasing the welding speed and placing the nozzle at the trailing position can decrease the upward momentum of the molten metal around the keyhole, and stabilize the keyhole, which are help to suppress the formation of spatter.

1. Introduction

The spatter which can be characterized as the ejection of melt from weld pool, is a general weld defect in laser welding [1]. The formation of spatter can also lead to other defects, such as underfill, undercuts. It is of great importance to study the formation mechanism of spatter, and adopt reasonable measures to reduce it.

Based on theoretical analysis of energy balance in laser welding, Semak suggested that the high-velocity -melt-flow ejection from the laser-metal interaction zone was induced by the recoil pressure [2]. Fabbro studied the droplet generation process in Nd-YAG continuous wave laser welding, and found that the droplet ejection locations were different in low and high welding speed [3]. A systematic description of the different types of spatter was presented in the study of Kaplan, the fundamental sequence of phenomena in spatter formation can be described as the following: local boiling-melt acceleration-redirection of fluid flow-accumulation of vertical momentum–droplet ejection [4]. Biffi proposed an innovative nozzle to reduce the spatter in titanium laser drilling [5]. Kawahito studied the penetration characteristics of 304 austenitic stainless steel plates with a 10 kW fiber laser beam, and found that the strong shear force of a laser induced plume can cause the generation of spatters [6]. Zhang used a modified "sandwish" specimen to observe the keyhole wall, vapor plume, and spatter formation, the spatter generation mechanisms at partial and full penetration laser welding processes were analyzed [7]. Li investigated the weld pool convection in the laser welding with the help of platinum and the X-ray imaging system, he proposed that the behavior of the weld pool was the key factor that influenced the spatter formation [8]. Liu studied the spatter behavior in the selective laser melting of AISI 316L stainless steel powder, and found that the energy input had an great influence on the spatter size, scattering state and jetting height [9].

In previous researches, investigation of spatter formation is heavily relied on experimental observation. It is clear that the spatter phenomenon is very complex, there are impediments to study the spatter generation entirely based on experiments. Hugger used the commercial software OpenFOAM to model the detachment of droplets in laser welding, but the behavior of the weld pool had not been discussed [10]. Chang built a CFD model to analyze the formation mechanism of spatter, and found that the occurrence of spatter was closely related to the flow velocity and vorticity in the weld pool, however the effect of keyhole was ignored in the model [11].

5083 aluminum alloy is widely used in modern high speed train and shipbuilding manufacturing industry, however the studies on spatter formation in 5083 aluminum alloy laser welding are very limited [10]. In this article, a three-dimensional numerical model

* Corresponding author at: Shanghai Key Laboratory of Material Laser Processing and Modification (Shanghai Jiaotong University), Shanghai 200240, PR China.
E-mail address: xmhua@sjtu.edu.cn (X. Hua).

http://dx.doi.org/10.1016/j.ijheatmasstransfer.2017.05.125
0017-9310/

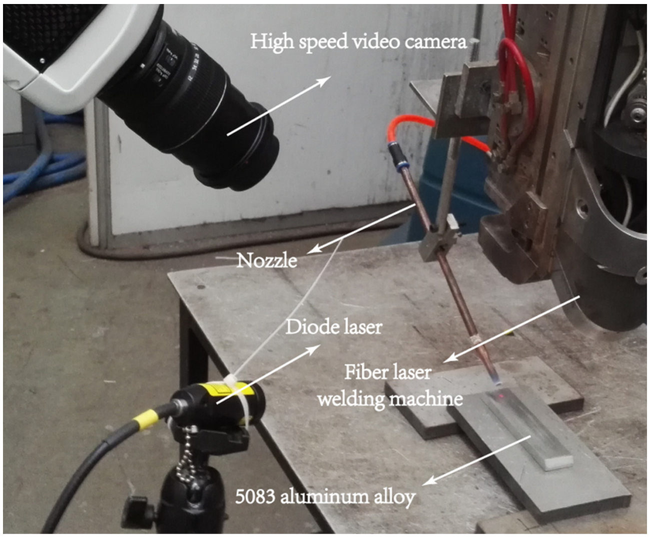

Fig. 1. The experimental platform.

is established to investigate the spatter formation in fiber laser welding of 5083 aluminum alloy, the shear stress caused by the metallic vapor flow that has great influence on spatter formation is considered, the effect of keyhole and the fluid flow features within the weld pool are discussed. The high speed photography system is used to capture the transient images of the weld pool and spatter. The results of this article could better clarify the spatter formation in fiber laser welding of 5083 aluminum alloy.

2. Experimental procedure

The experimental set-up used for the experiments is shown in Fig. 1. The experiments are performed using a fiber laser welding machine (IPG YLS-10,000), whose maximum output power is 10 kW, output wavelength is 1070 ± 10 nm, the focus radius is 0.36 mm. During the experiments, the laser power is 7 kW, the defocused distance is 0 mm, the welding speed is 2 m/min and 9 m/min, respectively, pure argon gas is used as shielding gas with a flow rate of 20 L/min, the nozzle is placed at the trailing position with a typical inclination of 45°. The material used is 10 mm-thick 5083 aluminum alloy, the thermo-physical material properties of the base metal is shown in Table 1. The top views of the weld beads are displayed in Fig. 2.

A high speed video camera is used to observe the weld pool behavior and spatter formation, a band pass filter with a transmission band of 808 nm is positioned in front of the camera lens to filter out unwanted arc light, the frequency is 2000 frame/s. In order to observe the weld pool, a diode laser (λ = 806 ± 10 nm) with a maximum power of 300 W is used to illuminate the welding zone.

3. The droplet escape condition

3.1. Young-Laplace equation

The surface tension pressure of a curved surface can be obtained from the Young-Laplace equation. As shown in Fig. 3, AB is a raised liquid surface, the radius is r, the perimeter of AB bottom surface is $2\pi r$, the area of AB bottom surface isπr^2, the radius of the sphere is R. The liquid surface tension is γ, the component in horizontal direction is$\gamma \sin\alpha$, the component in vertical direction is$\gamma \cos\alpha$, the sum of liquid surface tension in vertical direction is$\gamma \cos\alpha \cdot 2\pi r$. So the surface tension pressure of the raised liquid surface is$\Delta p = \gamma \cos\alpha \cdot 2\pi r/\pi r^2$. For $\cos\alpha = r/R$, so we can get:

$$\Delta p = \frac{2\gamma}{R} \tag{1}$$

The radius R needs to be considered in both dimensions at the surface location. If both radii are equal, this factor two appears. Otherwise it would be $(\gamma/R_1 + \gamma/R_2)$ for two different radii.

3.2. The droplet escape condition

The droplet escape condition is obtained by comparing the stagnation pressure of the liquid metal with the surface tension pressure of a curved surface. The magnitude of stagnation pressure can be derived from a simplified form of Bernoulli equation. For incompressible flow, $P_{stagnation} = \rho v^2/2$.

Where ρ is fluid density, v is the vertical component of the velocity, normal to the surface at a certain location.

When the stagnation pressure of the liquid metal is larger than the surface tension pressure, the droplets are generated. That is:

$$\frac{1}{2}\rho v^2 \geq \frac{2\gamma}{R} \tag{2}$$

4. Mathematical model and numerical simulation

Some assumptions have been made to simplify the mathematic model: (1) The flow is laminar, the liquid metal is considered to be a Newtonian and incompressible fluid. (2) The effect of shielding gas on welding process is omitted. (3) The heat source of laser beam is modeled as Guassian density distribution.

4.1. Governing equations

The weld pool simulation of laser welding is based on the numerical simulation of mass, momentum, and energy equations. The VOF (Volume of Fluid) method is used to trace the free surface deformation of the weld pool [12].

Mass conservation equation:

$$\nabla \cdot \vec{V} = 0 \tag{3}$$

Table 1
Thermo-physical material properties of 5083 aluminum alloy.

Nomenclature	Value	Nomenclature	Value
Density (l)	2380 (kg/m^3)	Thermal conductivity (s)	235 (W/m·K)
Density (s)	2660 (kg/m^3)	Liquidus temperature	933 (K)
Viscosity	4.2×10^{-3} (kg/m·s)	Solidus temperature	847 (K)
Specific heat (l)	1197.21 (J/kg·K)	Boiling temperature	2720 (K)
Specific heat (s)	1050 (J/kg·K)	Heat transfer coefficient	20 ($W/m^2 \cdot K^4$)
Latent heat of fusion	3.87×10^5 (J/kg)	Coefficient of thermal expansion	1.5×10^{-4} (K^{-1})
Latent heat of vapor	1.05×10^7 (J/kg)	Surface tension	0.871 (N/m)
Thermal conductivity (l)	90 (W/m·K)	Surface tension gradient	−0.000155 (N/m·K)